A Binocular Model to Evaluate User Experience in Ophthalmic and AR Prescription Lens Designs

Collins Opoku-Baah*
Heru Inc,
Clinical Development,
Miami, Florida, USA

Ian Erkelens†
Applied Perception
Science, Meta Reality
Labs, Redmond, WA, USA

Frank Qian‡
Applied Perception
Science, Meta Reality
Labs, Redmond, WA, USA

Robin Sharma§
Applied Perception
Science, Meta Reality
Labs, Redmond, WA, USA

ABSTRACT

Supporting refractive correction in head-mounted AR systems is central for providing accessibility across a diverse population. Importantly, matching the visual experience between a user's traditional ophthalmic lenses and their AR devices is critical for a seamless and comfortable user experience. In terms of geometric distortion, this can be challenging with the addition of optical and non-optical elements that accompany the AR experience. We developed an analytical model that quantifies the binocular aspects of optically induced geometric distortions with an aim to develop perceptually based metrics that can predict the user's experience with different spectacle lens designs. We anchored this model against empirical data collected from a small study where we systematically varied the front surface curvature of a user's habitual refractive correction. Importantly, the models we derived explained a significant amount of variance (r^2 = 0.46 to 0.92) in users' reported visual comfort. These results support the value of quantifying the binocular aspects of the visual experience in see-through optical systems and lay a foundation for a user-centric, quantitative system that can be used to evaluate optical lens designs in both the ophthalmic and near-eye display industries.

Keywords: binocular vision, augmented reality, user experience, ophthalmic prescription lens design, pupil swim, motion sickness, lens front surface curvature

Index Terms: Human computer interaction (HCI)–HCI design and evaluation methods–User studies; Computing methodologies–Modeling and simulation–Model development and analysis; Human-centered computing–Human computer interaction (HCI)–Interaction paradigms–Mixed / augmented reality

1 INTRODUCTION

Mixed (MR) and augmented reality (AR) head-mounted devices (HMDs) promise to revolutionize the way we consume and interact with information through the ability to seamlessly blend digital and physical spaces. As such, these emerging technologies have many real-life applications that span education, entertainment, communication, medicine, commerce, training, and research that might benefit society.

* e-mail: copokubaah@heru.net
† e-mail: ian.erkelens@fb.com
‡ e-mail: frank.qian@fb.com
§ e-mail: robin.sharma@fb.com

Designing wearable, mass-manufacturable technologies for the entire population for people of all ages, genders, abilities (e.g., visual), languages, cultures, and anthropometric differences is challenging. One important step towards achieving an inclusive user experience and improved wearability is to incorporate refractive correction into AR devices so that users who habitually wear glasses can enjoy the same experience as their non-glasses wearing counterparts. Indeed, it is estimated that by 2050, about 1 in 2 persons will be near-sighted (myopia) across the world [1]. These statistics indicate that many of the users of future AR HMD devices will require prescription glasses.

Designing prescription lenses is a complicated process as changes in some aspects of the optical architecture can influence the comfortable and seamless user experience desired for wearers. For instance, in the ophthalmic industry, anecdotal evidence suggests that changing the front surface curvature of a patient's existing prescription lens, even when the optical power remains the same, can induce symptoms of visually-induced motion sickness (VIMS) that arise from changes in geometric distortion that vary with pupil & gaze position [2], [3]–a phenomenon known as pupil swim in the head-mounted display industry [4]. The design process becomes more challenging when one aims to match the visual experience between a user's traditional ophthalmic lenses and their AR devices, due to the addition of other optical and non-optical elements within the see-through display stack that accompany the AR experience. In AR optical systems, prescription lens users may experience similar symptoms of motion sickness related to changes in the optical distortions that could result from any number of additional elements in the optical architecture. Furthermore, for a significant proportion of people, refractive prescription is different between the two eyes in terms of the spherical power, cylindrical power, and cylindrical axis [5], [6]. This difference in monocular prescriptions causes unequal monocular distortions when lens designs are altered and induces binocular disparities that can create depth perception and oculomotor problems [7]–[9].

The combined clinical wisdom and optical constraints that certain types of AR display architectures may impose on prescription lens design suggest a non-zero risk to users' initial experience, visual comfort, and eventual adaptation to an AR HMD system. Currently, there is a paucity of empirical studies or computational models to perceptually quantify this problem and provide metrics to guide optical design efforts. Our study sought to develop an analytical model that describes the binocular aspects of geometric distortions induced by changes in ophthalmic lens design in an ecologically valid way. We evaluated the performance of this model against pilot data collected from an empirical study conducted to perceptually quantify the impact of changes in front surface curvature of prescription lenses on the user experience through visual comfort assessment.

2 RELATED WORKS

2.1 Pupil swim in Ophthalmic Prescription glasses

Static images produced by devices that use viewing optics are subject to several aberrations including nonuniform distortion [10], [11]. In general, optically induced geometric distortion scales with increasing radial distance from the optical axis and is sensitive to eye position [12]. Changes in eye position relative to a lens system caused by eye or head movements can create dynamically changing distortions–also known as "pupil swim" [13].

Pupil swim is known to occur in prescription ophthalmic lenses. When changes in lens material (e.g., refractive index) or lens design occur (e.g., changing from single-vision lenses to multifocal lenses or changing the front surface curvature of the prescription's lens), pupil swim becomes an issue for the patient's visual comfort. For example, ophthalmic prescription lenses are typically designed to have a meniscus shape [14]. This shape is selected to ensure optimal image quality and visual acuity across eccentricity by minimizing marginal astigmatism and as a result, leaving geometric distortion to vary [15]. This approach assumes that it is possible for lens wearers to adapt to the perceptual effects of altered geometric distortion compared to that of marginal astigmatism which induces blur and reduces visual acuity. Typically, most patients adapt to the perceptual effects of distortion over time. Clinical dogma suggests that any patient experiencing pupil swim symptoms (visually induced motion sickness) should attempt to wear the new lenses full time for up to 2 weeks to allow for adaptation and, hopefully, symptom reduction. However, some patients are unable to adapt to the effects of pupil swim and this may contribute to higher rates of return of prescribed spectacle glasses in the ophthalmic industry.

2.2 The need for binocular vision inspired models of pupil swim in AR prescription lens design

A significant proportion of prescription lens wearers have unequal refractive errors (anisometropia) between the eyes and hence, require prescription powers that differ with respect to the spherical power, cylindrical power, and cylindrical axis [5], [6]. Unequal monocular spectacle prescriptions result in differences in magnification between the two eyes when the eyes are fixated at one point (clinically known as 'static aniseikonia') [8]. Because the eyes are constantly moving, gaze shifts in the presence of unequal monocular prescriptions result in differential optical prismatic deviations that require unequal compensatory vergence eye movements in order to fuse the images and avoid double vision (clinically referred to as "dynamic aniseikonia") [8]. Depending on the magnitude of the prescription difference, both static and dynamic aniseikonia create barriers to optimal binocular visual functions such as summation and stereopsis, while also causing symptoms such as headache, asthenopia (eye strain) and diplopia [7]–[9], [16]. Clinically, anecdotal evidence suggests that monocular vision (i.e., occluding one eye) helps relieve symptoms associated with pupil swim induced by unequal prescription power [17]. The presence of anisometropia and the ensuing static and dynamic aniseikonia support the notion that pupil swim in ophthalmic lenses is, in large part, a binocular vision problem. As such, perceptual and computational models aimed at quantifying VIMS due to optically induced geometric distortions should account for the binocular aspects of the problem.

3 MODEL DEVELOPMENT

A primary goal of this research was to develop an analytical modeling framework that describes the binocular aspects of dynamic distortion induced by changes in ophthalmic lens design.

3.1 Determining Retinal Projection Vectors for Eye Movement Simulations

Eye movements were simulated by rotating the aperture stop around the center of rotation of the eye, assumed to be located 13.5 mm behind the eye aperture. For this study, we simulated both horizontal and vertical vestibular-ocular response (VOR) eye movements and then sampled a number of gaze positions using a non-linear sampling procedure. By definition, the VOR eye movement is a compensatory eye movement that is generated to stabilize retinal image during head rotation [18]. When the head moves, the eyes counter-rotate at approximately the same speed but in the opposite direction [18]. VOR is known to be more sensitive to VIMS owing to the fact that the eyes are fixed while the pupil position with respect to the lens changes rapidly [4]. In our simulation, one revolution of the VOR eye movement begins with the two eyes fixated at a distance of 1m and the head located in the primary position. The two eyes are rotated leftward (i.e., for the horizontal eye movement) to an angle of 20 degrees at a velocity of ~450 degrees/sec (indicating that the head moved rightward), and then rightward at similar velocity and angle of rotation, and finally back to the center of fixation. For each temporally sampled gaze position during the eye movement (i.e., either horizontal or vertical), we determined the projection vectors for 1081 retinal points per eye sampled within an angular cone of 30 degrees of retinal space in radial and polar steps of 2 degrees and 5 degrees, respectively.

3.2 Horopter Surface Determination and Analysis

Next, to emphasize the binocular aspects of this phenomenon, we intersected corresponding retinal projections between the eyes to form a binocular surface separately for each sampled gaze point in the eye movement simulation. This binocular surface is termed as the horopter and in vision science, it serves as a tool for simplifying binocular vision geometry and thus, provides a useful avenue for analyzing and comparing different models of binocular distortion [19]. We fitted Zernike polynomials to describe basic shapes in the binocular horopter surface at each gaze point. Zernike polynomials present several advantages that make them suitable for our binocular horopter surfaces. First, the orthogonality of Zernike polynomials means that the individual terms are independent of one another and thus weighting of a finite set of terms does not depend on the presence or absence of other terms [20]. Second, unlike other polynomials, the shapes that are described by Zernike polynomials have similarities to the typical Seidel aberrations found in the eye [20], [21]. For example, while terms such as oblique astigmatism, spherical defocus, and vertical astigmatism relate to the clinical refractive errors that are corrected with prescription lenses, terms such as horizontal and vertical tilt describe quantitative changes in our horopter surfaces induced by prismatic effect and can therefore describe how a surface may be distorted from simple head and gaze shifts. In fact, most of these low-order Zernike terms resemble basic patterns of optic flow that the brain could interpret as biological motion and thus induce cue-conflict and VIMS. Collectively, these properties of Zernike polynomials make them a reasonable candidate suitable for describing how the binocular horopter surface will change based on

the ophthalmic lens design and eye movement patterns simulated in our model. For fitting, the second order Zernike polynomials constituting the first 6 terms were used: the zeroth order term, piston; the first order terms, vertical and horizontal tilt; and the second order terms, oblique astigmatism, spherical defocus, and vertical astigmatism. The selection of the second order polynomial was based on optimization procedures to determine the smallest Zernike polynomial order (which defines the number of terms and thus, model complexity) that will most reliably describe our binocular horopter surface (Supplementary figure 1). For each gaze position in a particular eye movement simulation, we determined coefficients for all six Zernike terms from the best-fit model to the binocular horopter surface corresponding to that gaze position. (See Supplementary figure 2 for plots of changes in coefficients for each Zernike polynomial term across gaze positions of a horizontal VOR eye movement for different ophthalmic lens designs – based on front surface curvatures – chosen from one participant in the user study cohort).

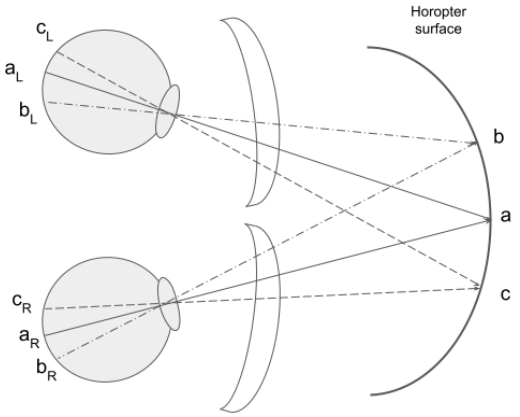

Figure 1: Determining Retinal Projection through Ray Tracing. Schematic depicts the scenario of the left and right eyes gazing through their respective spectacle lenses. Both eyes are fixating at a point in space, labeled as 'a'. The solid lines represent the trajectories of light from the fixation target to the locus of fixation of both eyes, labeled aL and aR. Schematic also shows two additional retinal locations per eye, labeled bR, bL and cR, cL respectively. Hypothetical rays are traced out from each corresponding to the angular eccentricities on the retina. The intersection of these rays in space is determined to be at points b and c. This process is repeated for multiple corresponding retinal locations on each eye to determine the horopter surface. This process is repeated for each instant in time sampled during a VOR eye-movement.

3.3 Deriving Metrics to Quantify Pupil Swim

Finally, we derived different metrics to quantify pupil swim induced by changes in ophthalmic lens design. As explained earlier, pupil swim may induce symptoms of VIMS through the generation of optic flow in features or scenes that conflict with vestibular cues during head and/or eye movements. Based on this notion, we hypothesized that symptoms of VIMS induced by changes in ophthalmic lens design may be predicted by eye movement induced changes in the measures of the horopter surface. For a particular participant, front surface curve configuration, and eye movement pattern (horizontal and vertical VOR), we derived 3 dynamic metrics–namely maximum-minimum coefficient, mean rate of change, and maximum rate of change. The maximum-minimum coefficient metric was determined as the difference between the maximum and minimum Zernike term coefficients selected across all the gaze positions.

$$maxmin_j = max\left[coefficients\ across\ all\ gaze\ positions_j\right] - min\left[coefficients\ across\ all\ gaze\ positions_j\right] \quad (1)$$

where j represents a Zernike polynomial term.

For the remaining metrics, we determined the gaze point to gaze point rate of change in Zernike coefficient across all gaze positions and then determined the mean or maximum rate of change.

$$rate\ of\ change_{ij} = \left[\frac{coefficient_{ij} - coefficient_{(i-1)j}}{time_i - time_{i-1}}\right] \quad (2)$$

$$mean\ rate\ of\ change_j = mean\left[rate\ of\ change_{(i=2,\ldots n)j}\right] \quad (3)$$

$$max\ rate\ of\ change_j = max\left[rate\ of\ change_{(i=2,\ldots n)j}\right] \quad (4)$$

where j represents a Zernike polynomial term and i represents gaze position.

For comparison, we derived a static metric that does not consider the effect of eye movements, and thus uses the value of the coefficient at primary gaze position as the measure for pupil swim for each ophthalmic lens design and eye movement. While the static model accounts for changes in the binocular horopter induced by 'static aniseikonia', the dynamic models are designed to evaluate the horopter changes induced by 'dynamic aniseikonia'.

4 USER STUDY

The aim of the user study was to subjectively quantify the impact of changes in ophthalmic lens design (specifically changes in front surface curvature) on user experience and comfort. The goal of this focused pilot study was to generate data from subjective evaluations of visual comfort to evaluate the performance of our pupil swim models.

4.1 Participants

Four prescription lens wearers (age ranged from 29 to 38 years, 1 female) participated in the user study. We were only able to recruit 4 participants for this pilot study due to the exacting nature of this experiment and the social-distance and remote work constraints imposed by COVID. Across these participants, the spherical component of their prescriptions ranged from -1.5D to -5D while the cylindrical component ranged from 0D to -2.25D, with varying degrees of anisometropia (Table 1). Informed consent was received from all subjects before participating in this study and all research protocols were evaluated and approved by our legal review board.

4.2 Procedure and Analysis

In this user study, our main independent variable was front surface curvature. We manipulated this variable by testing each participant on 7 lenses with different front surface curves ranging from 0.5D to 7.44D. However, due to lens edging and frame-mounting issues, not all participants were able to complete 7 lenses. Participants 1, 2, 3, and 4 completed 5, 7, 5 and 5 lenses respectively.

Table 1: Right and left eye prescriptions, and the nominal front surface curvature for participants enrolled in the study

Participant	Left Eye Prescription			Right Eye Prescription			Nominal Front Surface Curvature	
	Spherical Power	Cylindrical Power	Cylindrical Axis	Spherical Power	Cylindrical Power	Cylindrical Axis	Actual	Approximated
P1	-4.00	-1.00	165	-3.00	-0.75	170	3.60	4.47
P2	-1.75	0.00	000	-1.75	0.00	000	3.70	4.47
P3	-4.50	-0.50	180	-5.00	-0.25	090	2.75	1.52
P4	-1.50	-0.75	025	0.25	-1.00	165	8.00	7.44

Because we are interested in how deviation from participant's best or existing form lens can impact visual comfort, we determined for each participant their nominal front surface curvature by first measuring the front surface curvature of their habitual spectacles and finding the closest front surface curvature among the lenses tested by the participant to this nominal front surface curvature. Our dependent variable was the participants' subjective symptom rating on a vestibular oculomotor screening test (VOMS) [22], [23]. This test was designed to quantify the visual and physiological symptoms that may be related to motion sickness resulting from a head injury. The underlying theory is that oculomotor control and visual processing of optic flow is affected by a head-brain injury and the resulting retinal images that form during an eye movement do not match the system's expectations.

With each lens, participants performed an assessment of the VOMS in the comfort of their own home and in compliance with COVID related protocols at the time. In the test, participants were required to perform repetitions of different eye movements and rate their symptoms severity on a scale of 0-10 with 0 being no symptoms and 10 being severe symptoms. In our approach, we tested each lens on a separate day and also randomized the order of lens testing in order to minimize a possible confounding effect of lens order on our results. On a testing day, each participant performed repetitions of different eye movements described in the original VOMS test including both horizontal and vertical VOR tests and reported their symptom severity as well as baseline symptoms prior to testing. The testing always followed a particular order with smooth pursuits being first, followed by horizontal and vertical saccades and finally, horizontal, and vertical VORs. Clinically, these tests are arranged from weak to strong inducers of VIMS symptoms and under the assumption that symptom recovery may not be perfect and thus, performing a test that strongly induces VIMS symptoms first may affect the symptom rating of a subsequent test that weakly induces VIMS symptoms. Although all the eye movement tests were conducted, for this study, we focused our analysis on the VOR eye movement as studies have shown that VOR eye movements induce the worst symptoms compared to saccades and pursuits [22], [23].

During the subjective assessments, each participant was instructed to fixate a visual target approximately 1 meter ahead. To perform the horizontal VOR portion of the test, the head was rotated horizontally so that it reached an angular extreme of 20 degrees to the left at a speed of rotation of 180 beats/minute maintained using a metronome. One repetition is complete when the head moves back and forth to the starting position. After 10 repetitions were performed, participants immediately reported their symptoms rating on 6 symptoms namely: headache, dizziness, nausea, fogginess, eye strain and double vision. A similar approach was followed to perform the vertical VOR test. For each task, front surface curvature and participant, we determined the baseline-corrected symptom rating for each symptom (i.e., headache, dizziness, nausea, fogginess, eye strain and double vision) and then determined the sum of all the baseline-corrected ratings across symptoms.

$$summed\ baseline\ corrected\ symptom\ rating = \sum_{s=1}^{6}[symptom\ rating_{sk} - baseline\ symptom\ rating_s] \quad (5)$$

where s represents the type of symptoms and k represents the eye movement.

4.3 Results

Figure 2 shows plots of summed baseline-corrected symptom ratings as a function of deviation of lens front surface curvature from the determined nominal front surface curvature (see section 4.2) for each VOR eye movement (i.e., horizontal in red, vertical in blue) and participant (P1, P2, P3, P4). 2 out of 4 participants (P2 and P4) showed a trend of worsening symptoms as front surface curvature deviated from the nominal form. While participant P2 exhibited a trend of worsening symptoms for both flatter (negative) and steeper (positive) front surface curvatures, participant P4 only showed the trend for flatter front surface curvatures due to a high nominal front surface curvature and hence the absence of steeper front surface curvatures. Conversely, participants P1 and P3 showed trends that were variable and somewhat inconsistent with our proposed hypothesis. While participant P1 showed no consistent trend of either worsening or decreasing symptoms with flatter front surface curvatures, it appeared that participant P3 was not significantly affected by changes in front surface curvature. Comparing across participants, summed baseline-corrected symptoms ratings were comparable between horizontal and vertical OR, except for subject P3 where symptom ratings were slightly higher for horizontal compared with vertical VOR.

5 MODEL EVALUATION

Next, we determined how well the metrics derived from each model predicted the symptoms rating data obtained from the user data. For each metric (e.g., static), we employed a multiple linear regression model whose equation is as follows:

$$S_i = \beta_0 + \sum_{j=1}^{k}(\beta_j * Z_i^j) + \varepsilon_i \quad (6)$$

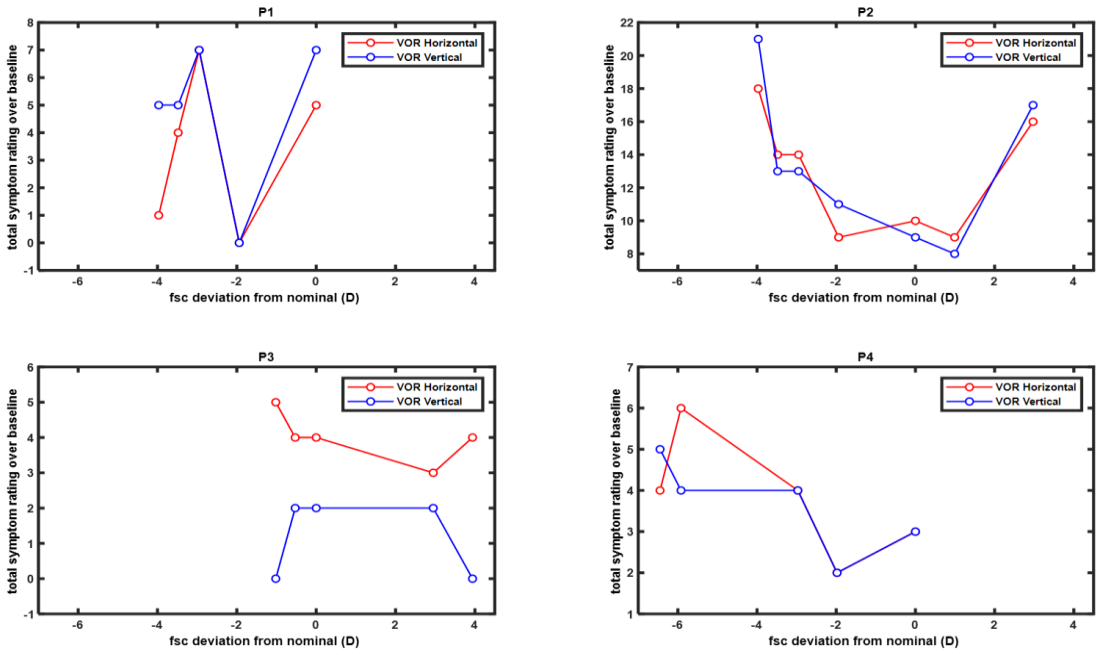

Figure 2: User study results. Plots showing deviations of front surface curvature from nominal in diopters (D) on the x-axis and total symptoms rating over baseline on the y-axis for both horizontal (red) and vertical (blue) VOR eye movement for each participant (P1, P2, P3 and P4). fsc: front surface curvature. Negative diopters on the x-axis correspond to flatter front surface curvatures, while positive values correspond to steeper curvatures

Since we were interested in predicting the change in user experience (i.e., symptoms rating) following a change in front surface curvature, S represented the summed baseline-corrected symptoms rating of a particular lens normalized to the summed baseline-corrected symptoms rating of the nominal front surface curvature for each participant. Likewise, Zj represented the metric value of a particular lens normalized to that of the nominal front surface curvature for a Zernike polynomial term j. Because we used the second order Zernike polynomial model, k equaled 6 and included the following terms: piston, vertical tilt, horizontal tilt, oblique astigmatism, spherical defocus, and vertical astigmatism. $\beta 0$ represented the y-intercept term, ε represented the error term, and βj represented the regression coefficient for each of Zernike polynomial terms. Normalizing the symptoms data and the metrics data of the various lenses to those of the nominal front surface curvature for each participant reduced the individual variability across participants, thus we pooled data points across participants and lenses. We assumed that the main source of variability across the data points stemmed from differences in front surface curvature. Moreover, because across participants most of the lenses used had front surface curvatures that were flatter than the respective nominal lenses, we included only the flatter lenses in the model evaluation. Therefore, the ith term represented an observation for a particular participant and a flatter front surface curvature. The coefficient of determination (R-squared) was used to measure how much of the variation in normalized symptom ratings could be explained by the variation in the independent variables.

Table 2 shows the r-squared goodness of fit values for the various models for both horizontal and vertical VOR eye movements. In general, the r-squared values across our models for both tasks ranged from 0.46 to 0.92 indicating that the metrics derived from the various models could explain a significant portion of the variability in the symptoms data. For the horizontal VOR task, only the linear model based on static (i.e., primary position) metric showed a statistically significant fit to the data ($r = 0.77$, $p = 0.049$) although that r-squared value for the linear model based on maximum rate of change metric ($r = 0.76$, $p = 0.058$) was comparable to that of the static metric. On the other hand, for the vertical VOR task, all the linear models except the model based on the static metric exhibited statistically significant fits to the data ($r>0.78$, $p < 0.044$). While the best model for the horizontal VOR was the static model, for vertical VOR, the best model was the maximum-minimum coefficient model.

6 DISCUSSION

In this study, we designed and evaluated analytical models for pupil swim that consider the binocular aspects induced by changes in ophthalmic lens design in spectacle lens wearers. To evaluate these models, we conducted a user study to perceptually quantify the impact of changes in prescription lens front surface curvature on user's visual comfort. In general, we observed a large degree variability in the subjective evaluations across the participants. Indeed, this finding is consistent with the report of significant variability in individual susceptibility to VIMS in HMD. Although our findings were not homogenous across participants, we found that 50% of our participants showed trends that were consistent with this hypothesis. This indicates that changing the front surface curvature of the user's optical prescription can negatively affect

Table 2: Modeling Results. r-squared goodness of fit values as well as p values for the different models for both horizontal and vertical VOR eye movements. Red highlighted figures represent fits that were statistically significant, i.e., $p < 0.05$.

VOR Task		primary position	Max-min coefficient	Mean rate of change	Max rate of change
Horizontal	**R^2**	**0.77**	0.46	0.49	0.76
	p-value	**0.049**	0.5	0.446	0.058
Vertical	**R^2**	0.71	**0.92**	**0.78**	**0.84**
	p-value	0.097	**0.002**	**0.044**	**0.016**

their visual comfort and user experience in a significant number of potential users. Importantly, our results suggest that metrics derived from fundamental visual perception principles–namely binocular vision, can explain a significant proportion of the variability in user visual comfort that arise from changes in their spectacle lens design.

7 CONCLUSION

Incorporating optical prescriptions into AR systems expose some risk to the user experience due to the challenges associated with matching the best form lenses of all prescriptions and the presence of unequal monocular prescriptions among potential users. Our study sets a great foundation for designing perceptual studies that quantify the impact of changes in ophthalmic lens design on wearers' comfort and experience, and models that consider the binocular aspects of pupil swim induced by these changes.

ACKNOWLEDGEMENT

We are thankful to James Hillis, Marina Zannoli, Jerry Jia and Teric Chan for their insightful discussion and contribution to development of ideas for this project.

REFERENCES

[1] B. A. Holden *et al.*, "Global prevalence of myopia and high myopia and temporal trends from 2000 through 2050," *Ophthalmology*, vol. 123, no. 5, pp. 1036–1042, 2016.

[2] "All About That BASE (CURVE)." https://www.2020mag.com/article/all-about-that-base-curve (accessed Jun. 03, 2022).

[3] P. Walker, "The Truth About Base Curves", Accessed: Jun. 03, 2022. [Online]. Available: https://www.abo-ncle.org/images/walker.pdf

[4] T. T. Chan, Y. Wang, R. H. Y. So, and J. Jia, "Predicting Subjective Discomfort Associated with Lens Distortion in VR Headsets During Vestibulo-Ocular Response to VR Scenes," *IEEE Trans. Vis. Comput. Graph.*, 2022.

[5] J. de Vries, "Anisometropia in children: analysis of a hospital population," *Br. J. Ophthalmol.*, vol. 69, no. 7, pp. 504–507, 1985.

[6] L. M. Almeder, L. B. Peck, and H. C. Howland, "Prevalence of anisometropia in volunteer laboratory and school screening populations," *Invest. Ophthalmol. Vis. Sci.*, vol. 31, no. 11, pp. 2448–2455, 1990.

[7] A. Remole, "Effect of induced dynamic aniseikonia on fixation performance during oblique gaze," *Optom. Vis. Sci. Off. Publ. Am. Acad. Optom.*, vol. 67, no. 1, pp. 13–18, 1990.

[8] A. Remole, "Anisophoria and aniseikonia. Part I. The relation between optical anisophoria and aniseikonia," *Optom. Vis. Sci. Off. Publ. Am. Acad. Optom.*, vol. 66, no. 10, pp. 659–670, 1989.

[9] A. Remole, "Anisophoria and aniseikonia. Part II. The management of optical anisophoria," *Optom. Vis. Sci. Off. Publ. Am. Acad. Optom.*, vol. 66, no. 11, pp. 736–746, 1989.

[10] J. P. Rolland and T. Hopkins, *A method of computational correction for optical distortion in head-mounted displays*. Citeseer, 1993.

[11] W. Robinett and J. P. Rolland, "A computational model for the stereoscopic optics of a head-mounted display," in *Virtual reality systems*, Elsevier, 1993, pp. 51–75.

[12] E. Hecht, "Optics 3rd ed., 330," 1998.

[13] Y. Geng *et al.*, "Viewing optics for immersive near-eye displays: pupil swim/size and weight/stray light," 2018, vol. 10676, p. 1067606.

[14] M. Jalie, "Ophthalmic Lenses & Dispensing 3rd Edition Butterworth Heinemann Oxford UK," 2008.

[15] J. Schwiegerling, "Field guide to visual and ophthalmic optics," 2004.

[16] D. M. Levi, S. P. McKee, and J. A. Movshon, "Visual deficits in anisometropia," *Vision Res.*, vol. 51, no. 1, pp. 48–57, 2011.

[17] T. E. Fannin and T. Grosvenor, *Clinical optics*. Butterworth-Heinemann, 2013.

[18] A. M. Wong, "Listing's law: clinical significance and implications for neural control," *Surv. Ophthalmol.*, vol. 49, no. 6, pp. 563–575, 2004.

[19] K. M. Schreiber, D. B. Tweed, and C. M. Schor, "The extended horopter: Quantifying retinal correspondence across changes of 3D eye position," *J. Vis.*, vol. 6, no. 1, pp. 6–6, 2006.

[20] V. Lakshminarayanan and A. Fleck, "Zernike polynomials: a guide," *J. Mod. Opt.*, vol. 58, no. 7, pp. 545–561, 2011.

[21] G. Conforti, "Zernike aberration coefficients from Seidel and higher-order power-series coefficients," *Opt. Lett.*, vol. 8, no. 7, pp. 407–408, 1983.

[22] A. Mucha *et al.*, "A brief vestibular/ocular motor screening (VOMS) assessment to evaluate concussions: preliminary findings," *Am. J. Sports Med.*, vol. 42, no. 10, pp. 2479–2486, 2014.

[23] S. Russell-Giller, D. Toto, M. Heitzman, M. Naematullah, and J. Shumko, "Correlating the King-Devick test with vestibular/ocular motor screening in adolescent patients with concussion: a pilot study," *Sports Health*, vol. 10, no. 4, pp. 334–339, 2018.